Lunar Measurements with OCI[1] during the PACE[2] Mission

1: Ocean Color Instrument
2: Plankton, Aerosol, Cloud, ocean Ecosystem

Gerhard Meister, PACE/OCI Instrument Scientist

NASA Code 616, United States

GSICS Annual Meeting 2024

Darmstadt, Germany; March 12th, 2024

OCI Hardware (from U. Gliese, IGARSS 2023)

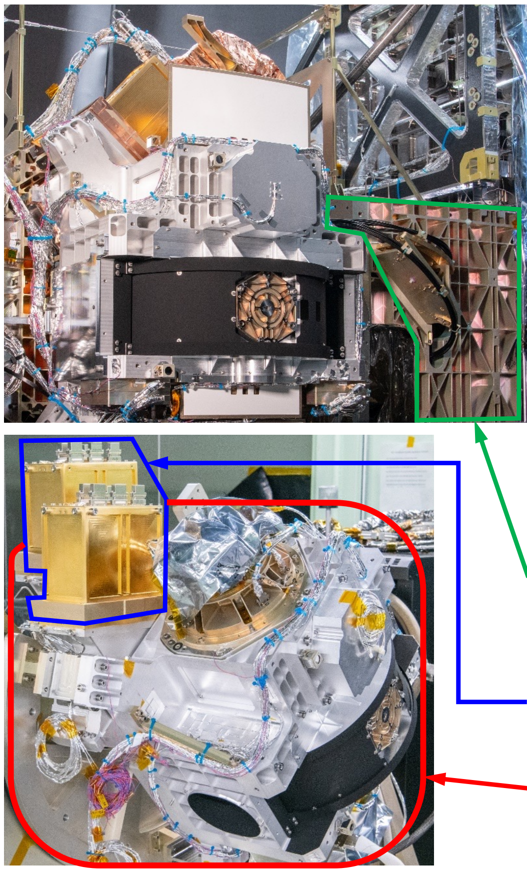

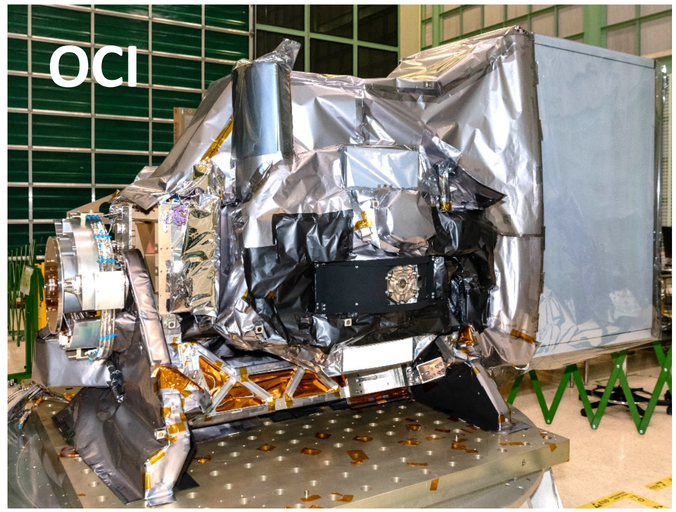

Fiber-Coupled 7-Band SWIR Detection System

Hyperspectral UVNIR Detection System

Hyperspectral Optical System

OCI image acquisition

- OCI is a rotating scanner, similar to SeaWiFS and VIIRS (rotating telescope and half angle mirror); rotation rate is 5.7Hz
- Image is acquired via motion of spacecraft in earth view mode (see picture below)
- Image is acquired via rotation of the spacecraft for lunar measurements

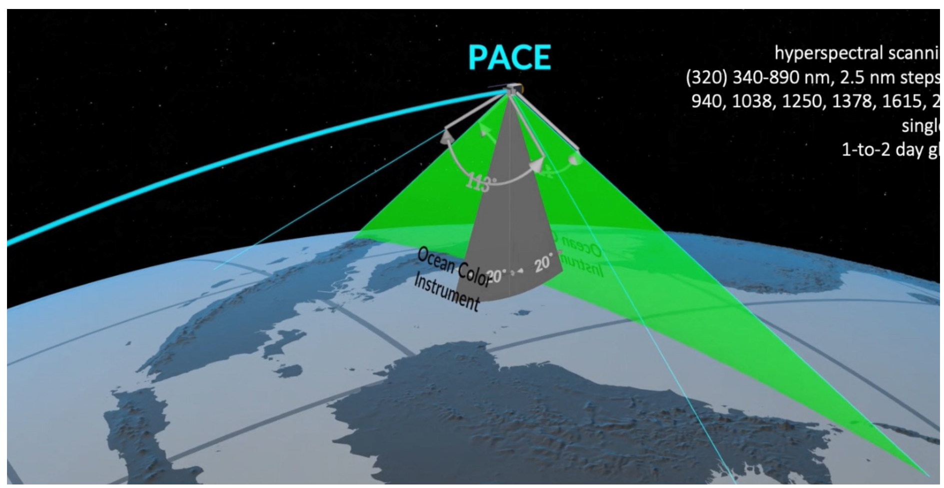

Image from U. Gliese, IGARSS 2023. See backup for full citations.

OCI Optical System (from U. Gliese, IGARSS 2023)

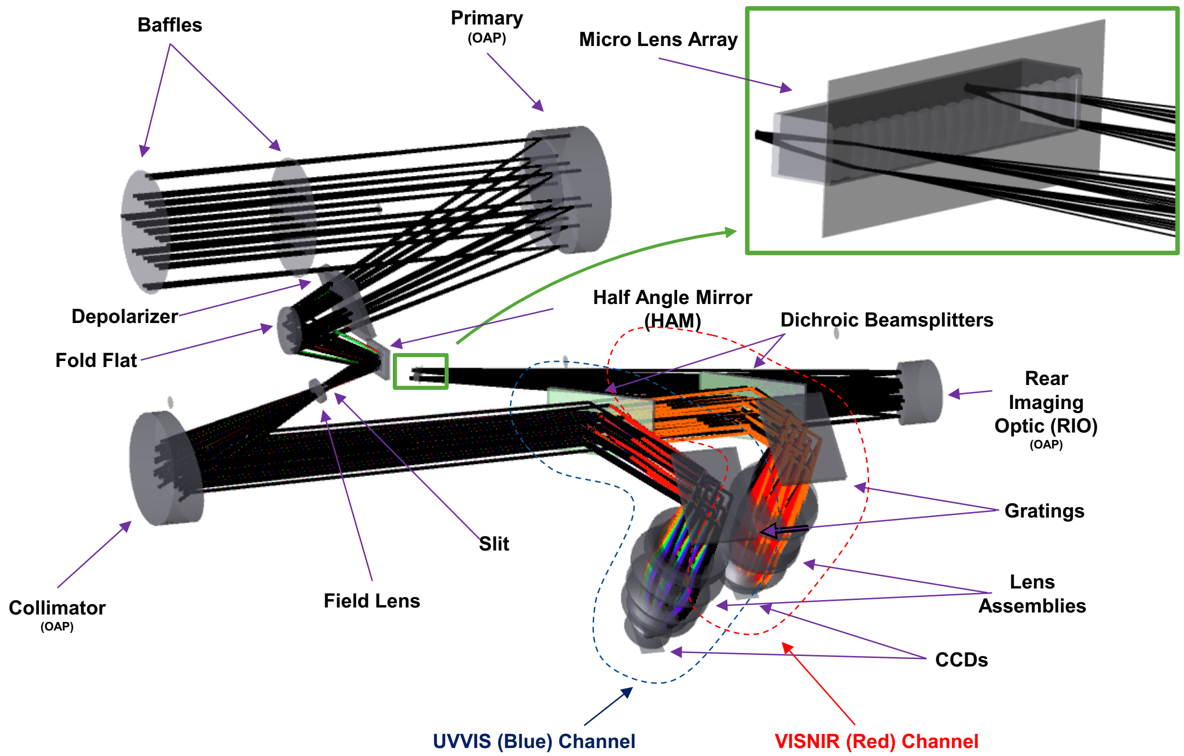

Signal is acquired via time-Delay Integration (TDI) in scan direction (16:1 for CCDs, 8:1 to 2:1 for SWIR bands)

OCI Spatial Performance (GSD, IFOV, FoR)

- Ground Sampling Distance (GSD) along scan/track: 0.0888deg/0.0881 deg (distance between pixel centers)
- Instantaneous Field of View (IFoV) along scan/track: 0.0889deg/0.0929deg (area imaged by a pixel)
- Effective spatial resolution for PACE orbit including 20deg tilt at 'nadir': **1.2km** (similar to SeaWiFS, larger than MODIS (1km))
- A lunar image will be about 7-8 1km pixels wide in scan direction (up to 32 in track direction due to oversampling) for the SWIR bands; bands below 900nm are acquired at 125m spatial resolution in scan direction (1km in track direction)

OCI Tilting on Spacecraft (from J. Knuble, IGARSS 2023)

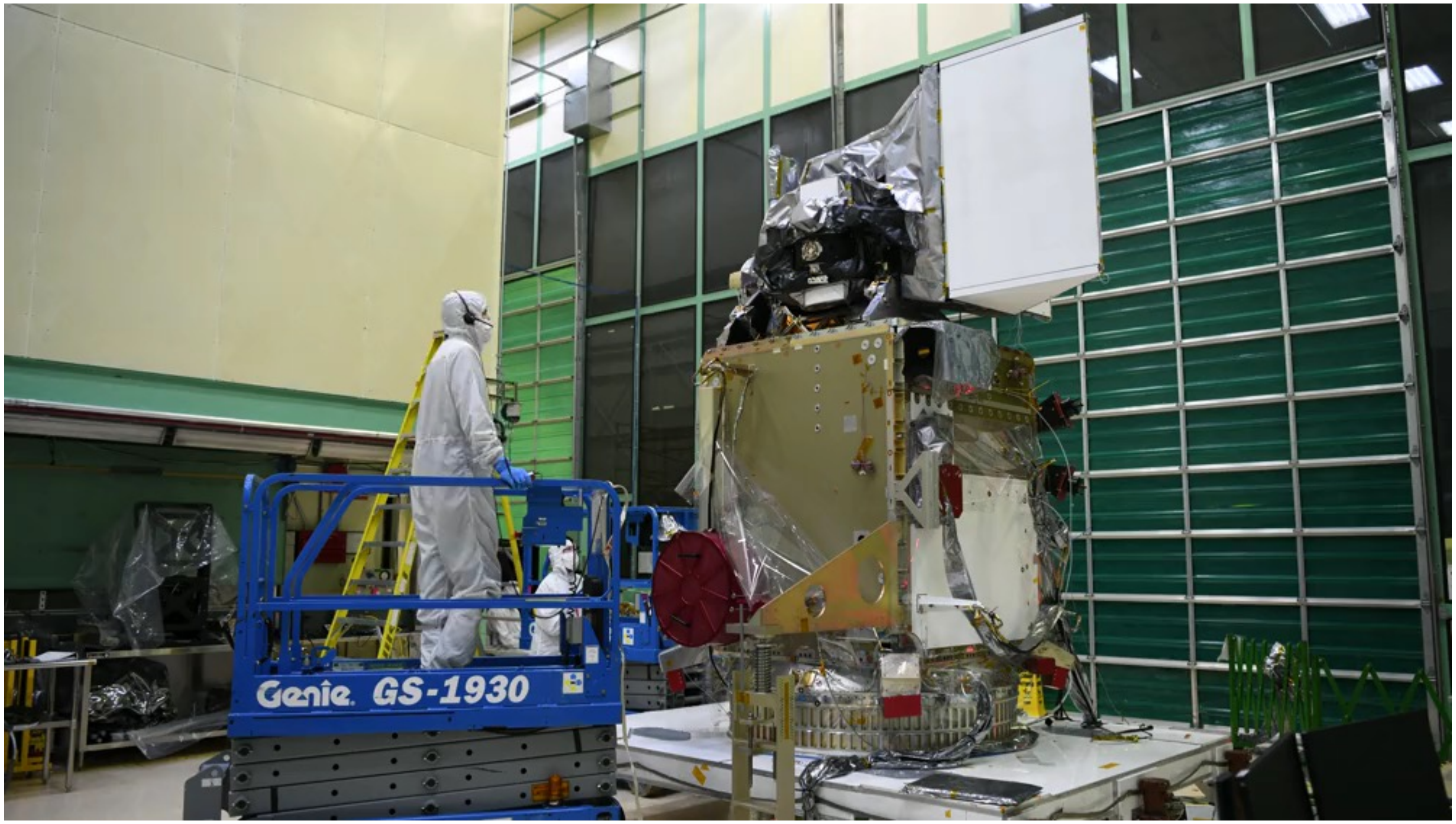

OCI on-orbit calibration

Radiance Calibration Equation

$$Lt = K1*K2(t)*(1-K3(T-Tref))*K4(\theta) *K5(dn)*Kp*dn$$

- Lt = Radiance, unit: W /(m^2 µm sr)
- K1 = absolute gain factor; unit: (W /(m^2 µm sr))/dn
- K2(t) = relative gain factor as a function of time t; unitless
- K3 = temperature correction [(deg $C)^{-1}$] (vector)
- T = Temperatures measured at relevant locations [deg C] (vector)
- Tref = Reference Temperature [deg C]
- θ =scan angle [deg]
- K4 = (θ) response versus scan ; unitless
- K5 = nonlinearity factor ; unitless
- dn = dark-corrected instrument counts

Kp: polarization correction applied in Level-2 code (correction needs TOA radiance polarization information)

Slide from G. Meister, IGARSS 2023.

K1, Kp and K3-K5 have been derived for all bands

- K2 will be derived on-orbit from solar diffuser and lunar measurements

- K1 will be updated with solar diffuser measurements

Solar Diffuser

- Daily/monthly for short/medium term (up to 2 years) tracking of radiometric gain changes
- 3 diffusers (2 bright, one dim for linearity) mounted on a 3-sided wheel, see picture
- Long term tracking via lunar irradiance measurements

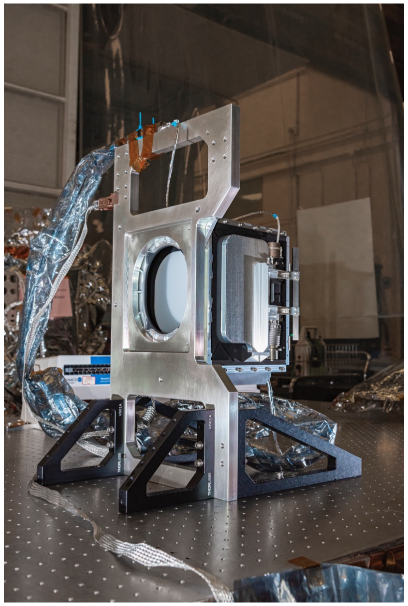

Lunar measurements

- OCI will measure lunar irradiance twice a month, at +/- 7deg phase angle during the dark side of the orbit via a pitch/slew/roll maneuver
- OCI LOS will be steered a few degree below the moon, slowly sweep across the moon, stop, and slowly sweep back (i.e. 2 lunar irradiance measurements
- Sweep speed will be highly controlled (oversampling factor of 4)

- Additionally, OCI will move its LOS to the center of the moon and stare for ~30 seconds to acquire a scan line with a high contrast signal for SWIR band characterization

OCI radiometric gain trending: approach

- First daily and monthly solar diffuser measurement provide K1
- Subsequent daily solar diffuser calibrations provide initial gain trend (K2)
- Subsequent monthly solar diffuser calibrations provide estimate of solar diffuser reflectance degradation as a function of solar exposure; if significant, K2 will be rederived with solar diffuser reflectance as a function of time
- After about 2 years, we expect our lunar time series to be accurate enough to provide corrections to the K2 trend (e.g. via a linear or an exponential adjustment)

OCI prelaunch calibration

Radiance Calibration Equation

$$Lt = K1*K2(t)*(1\text{-}K3(T\text{-}Tref))*K4(\theta) *K5(dn)*Kp*dn$$

- Lt = Radiance, unit: W /(m^2 µm sr)
- K1 = absolute gain factor; unit: (W /(m^2 µm sr))/dn
- K2(t) = relative gain factor as a function of time t; unitless
- K3 = temperature correction [(deg C)$^{-1}$] (vector)
- T = Temperatures measured at relevant locations [deg C] (vector)
- Tref = Reference Temperature [deg C]
- θ =scan angle [deg]
- K4 = (θ) response versus scan ; unitless
- K5 = nonlinearity factor ; unitless
- dn = dark-corrected instrument counts

Slide from G. Meister, IGARSS 2023.

Kp: polarization correction applied in Level-2 code (correction needs TOA radiance polarization information)

-K1, Kp and K3-K5 have been derived for all bands

- Signal to noise ratio (SNR) and Relative Spectral response (RSR) as well

GLAMR Test Video (from J. Knuble et al., IGARSS 2023)

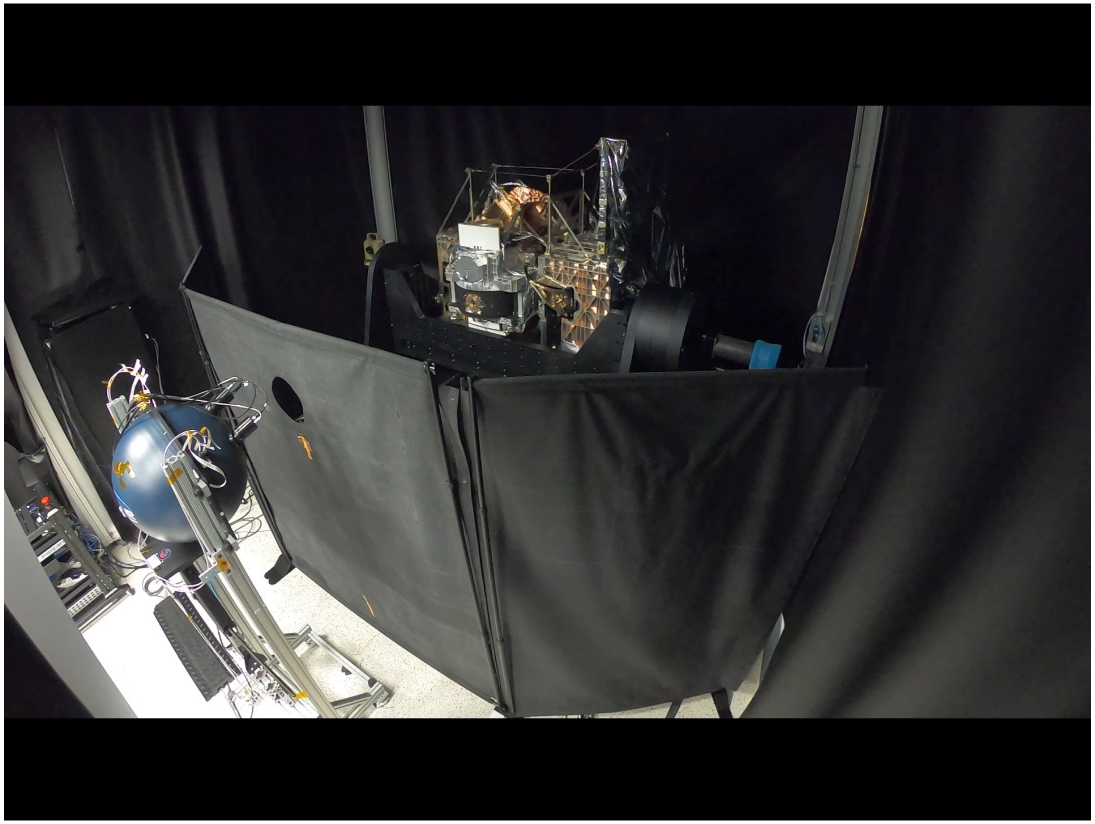

Hyperspectral bands: spectral coverage

- Blue FPA baseline aggregation: 119 L1B bands from **314.9nm to 605.7nm**
  - 116 L2 bands up to 598.3nm
  - Bands below 340nm have reduced radiometric accuracy (TBD on-orbit)
  - Bandwidth: ~5.1nm
- Red FPA baseline aggregation: 163 L1B bands from **600.5nm to 894.6nm**, bandwidth ~5.0nm
- 9 SWIR bands at 7 wavelengths from **940nm to 2260nm**

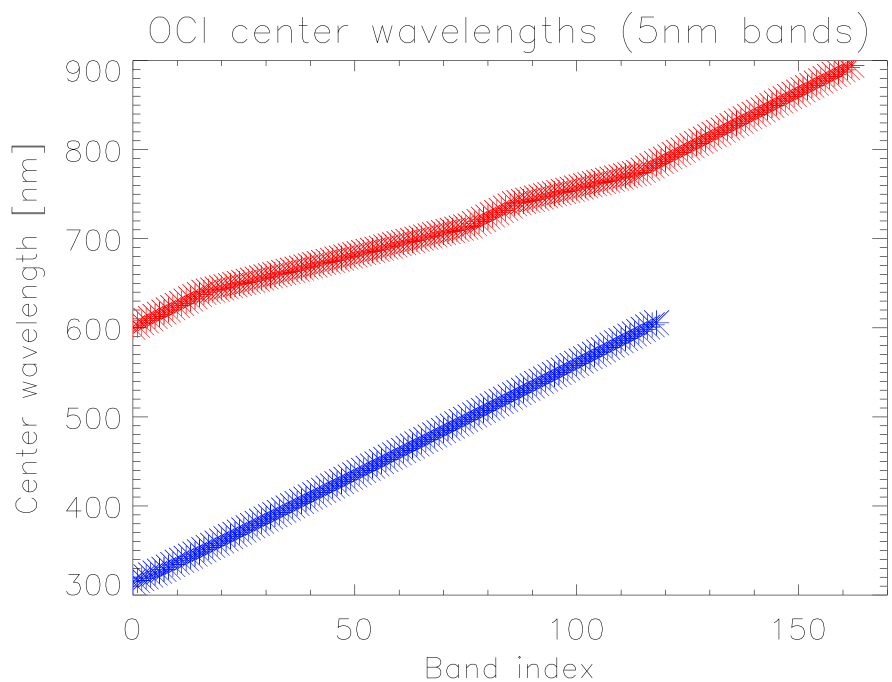

Slide from G. Meister,
IGARSS 2023.

K1 (gain), dispersion, bandwidth, out-of-band

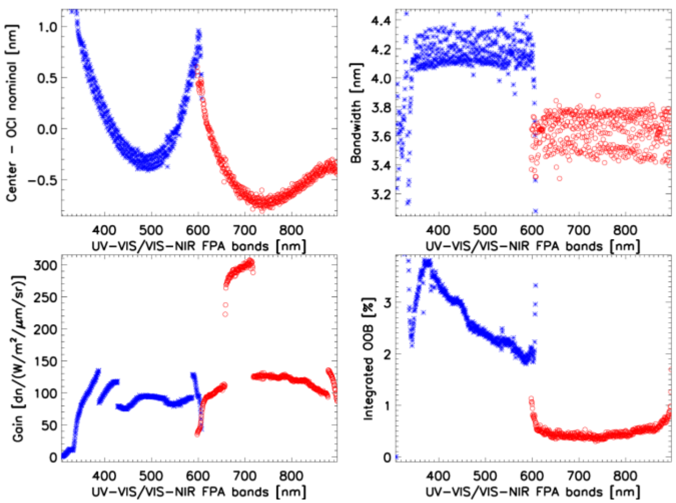

Figure 4. Results for all UV-VIS (blue stars) and VIS-NIR (red circles) FPA bands. Top left plot shows the spectral dispersion as the difference from the measured center wavelengths to the nominal center wavelengths of each band. Top right shows the bandwidth for each band. Bottom left shows the measured absolute system gain. Bottom right shows the integrated out-of-band response ratio.

Table 1. SWIR measured center wavelength, bandwidth, integrated OOB response ratio, and absolute system gain (SG: standard gain; HG: high gain).

Band Name	Center [nm]	FWHM [nm]	IOOB [%]	Gain [dn/(W/m2/ sr/um)]
940 SG	939.7	44.3	0.20	448
1038 HG	1038.3	74.4	0.13	2028
1250 SG	1250.4	28.5	0.16	684
1250 HG	1248.5	28.6	0.13	5494
1378 SG	1378.2	14.4	0.19	763
1615 SG	1619.6	73.7	0.11	1571
1615 HG	1618.0	73.6	0.11	12186
2130 SG	2130.6	49.3	0.12	4652
2260 SG	2258.4	72.8	0.18	6440

Figure and table taken from Kitchen-McKinley et al., PACE OCI Flight Unit Prelaunch Spectral Characterization, IGARSS 2023, Pasadena, CA.

OCI relative spectral response: blue and red FPA

- More RSR variation (electronic crosstalk) on red FPA, but at very low level (often negative)
- Decline from peak to <1e-3 much faster than in blue FPA
- Ghosts much smaller than in blue FPA

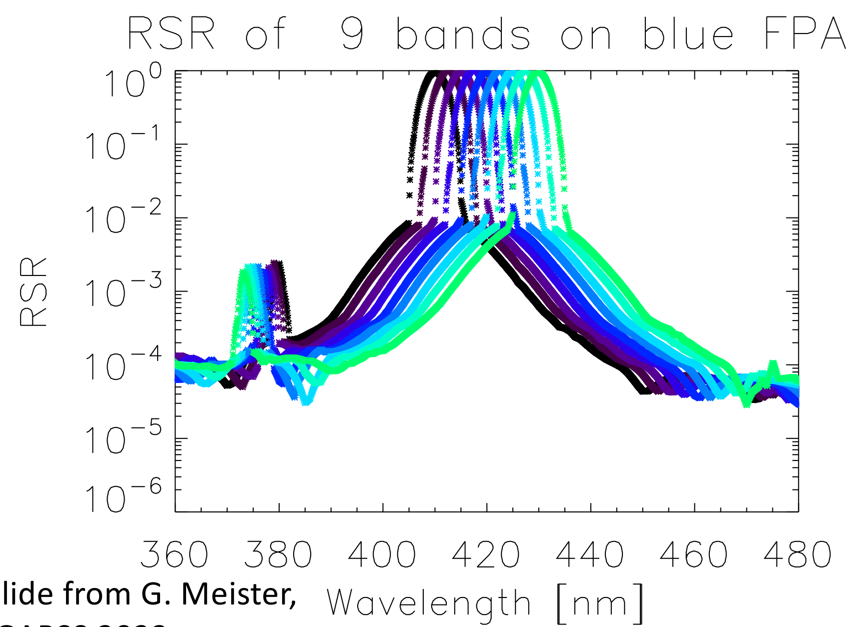

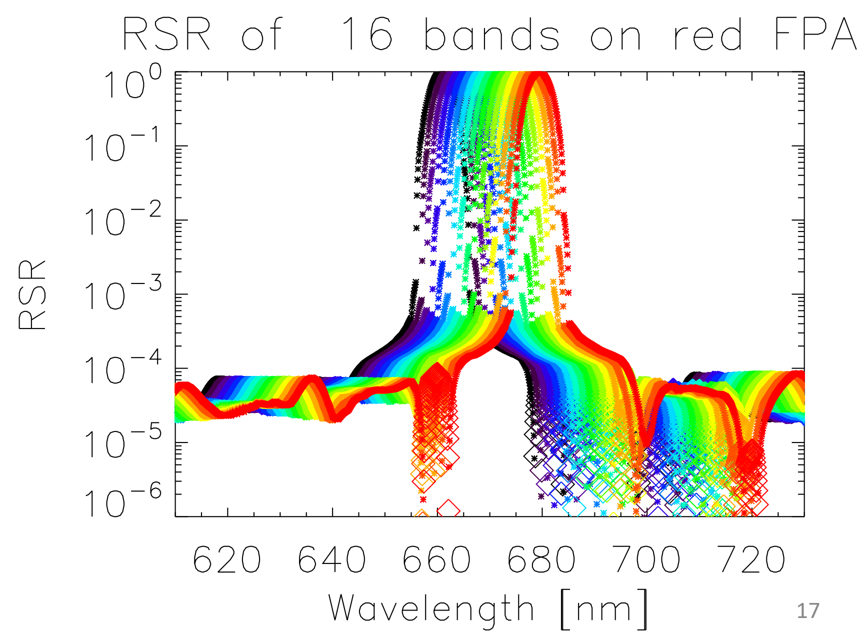

Slide from G. Meister, IGARSS 2023.

SNR Evaluation

SNR (412 nm and 555 nm)

Measured SNR plotted versus radiance (different lamp levels).

Data – symbols; Colors – TVAC temperatures (nominal, hot op, cold op)

Solid lines – Fit to data; Dashed vertical lines – TOA radiance levels (from requirements)

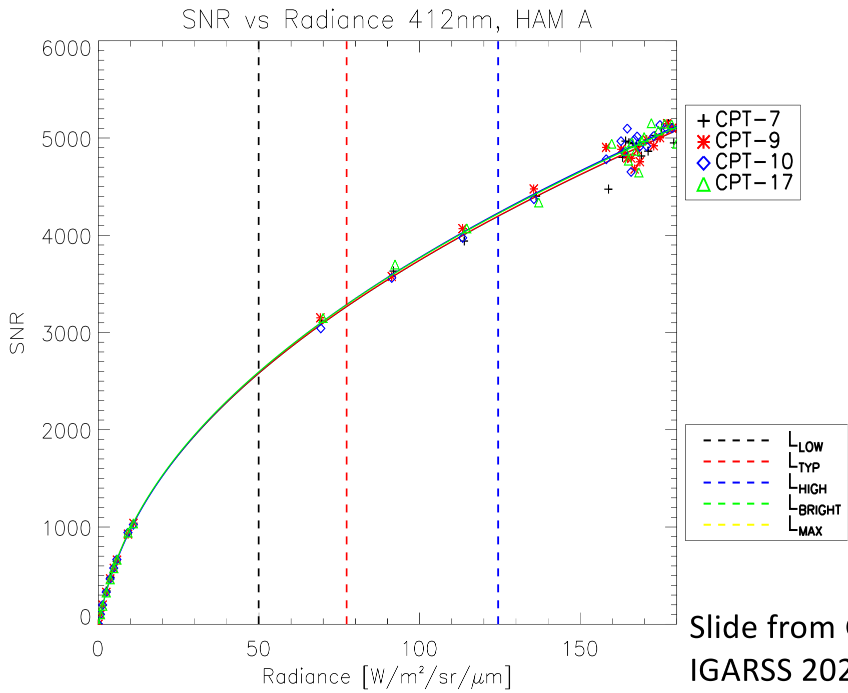

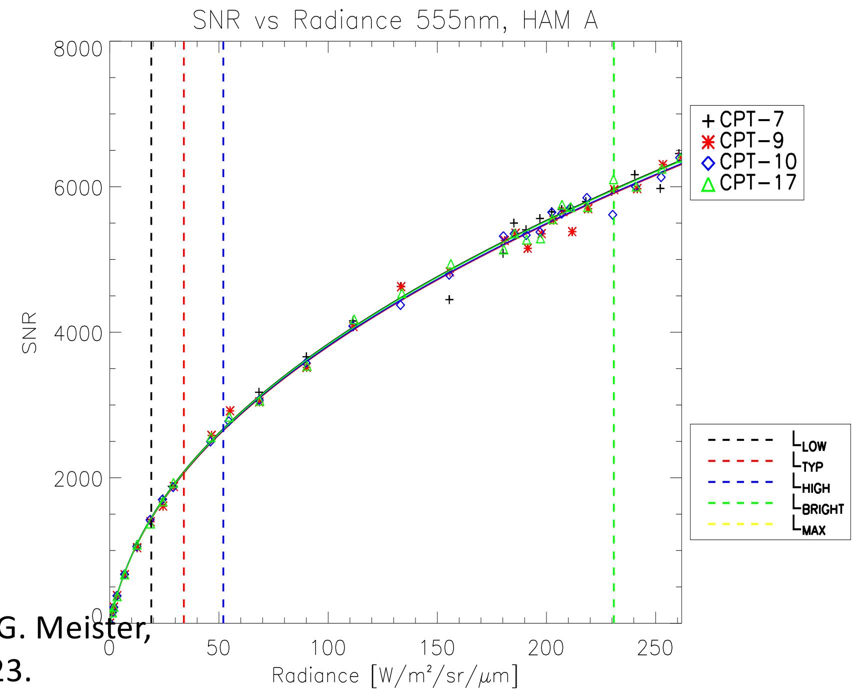

Slide from G. Meister, IGARSS 2023.

SNR at ocean L_{TYP} for hyperspectral bands

Very high SNR for hyperspectral bands (spectral aggregation needed above 800nm).
SNR for lunar radiances will be lower in the blue, higher in the red => sufficient for lunar analysis

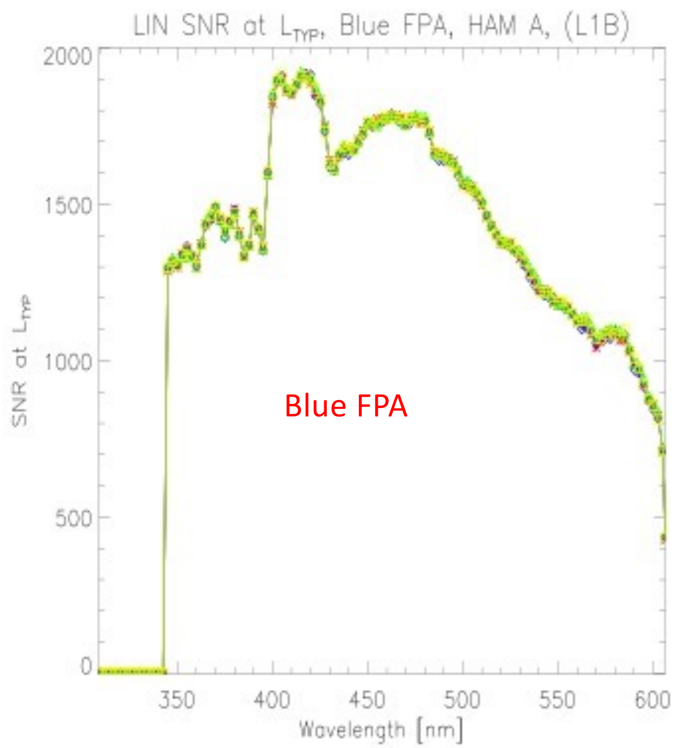

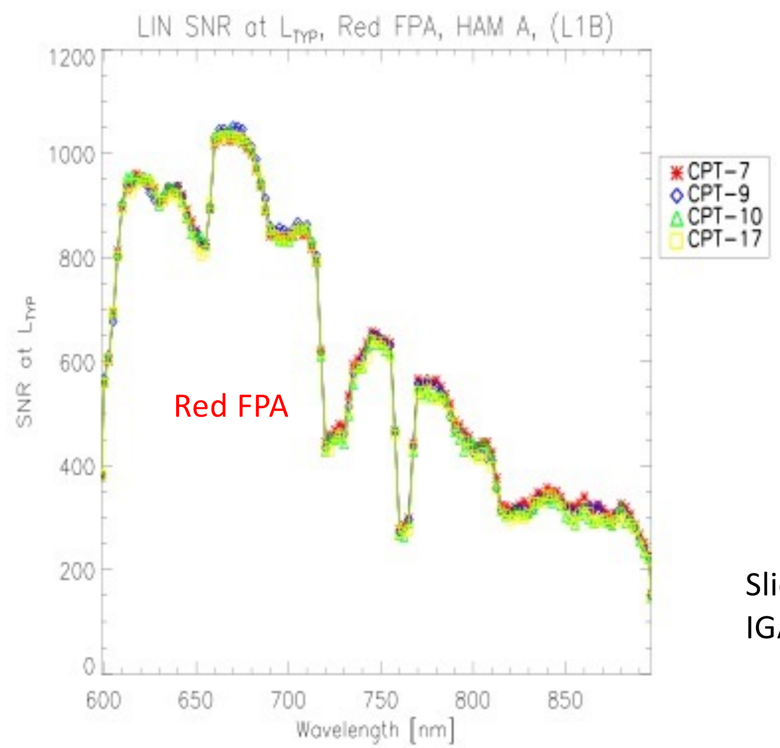

Slide from G. Meister, IGARSS 2023.

Kp: Polarization Sensitivity

Polarization amplitude measured at different scan angles

- Amplitude generally less than 0.4 % except in UV (below about 350 nm)
- Oscillations in red FPA a feature of the depolarizer
- Phase angle also determined – Mueller matrix components derived from amplitude and phase

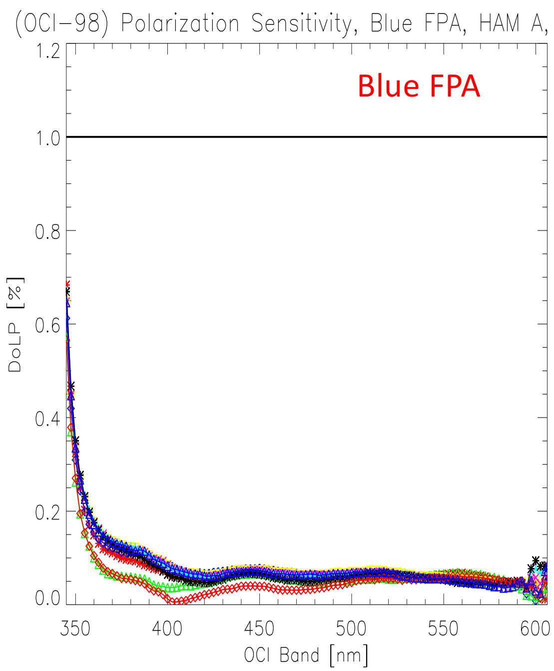

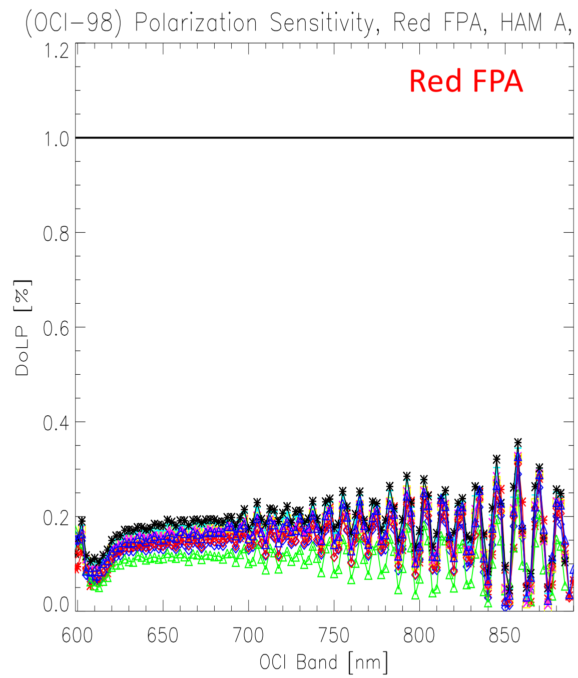

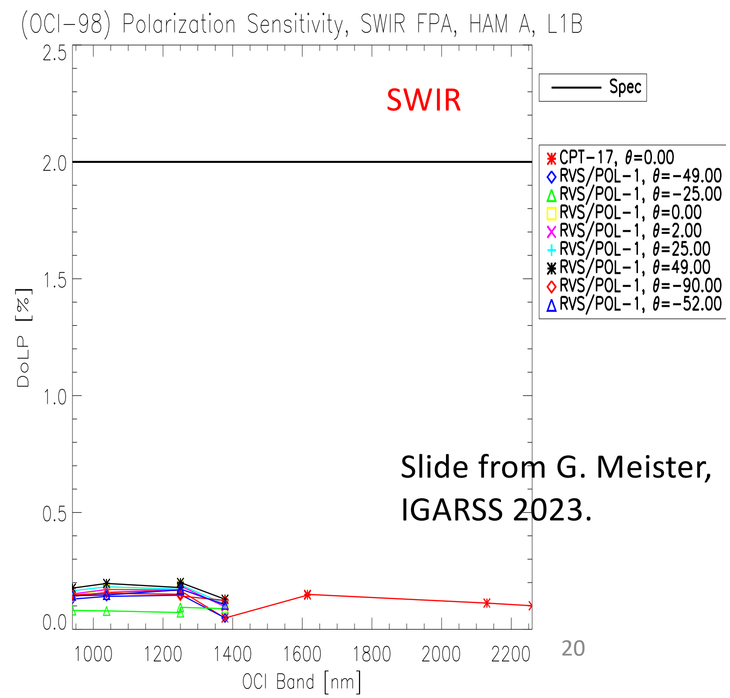

Slide from G. Meister, IGARSS 2023.

Saturation

- Saturation above L_{MAX} (or L_{CLIP}) for most bands, indicating expected science data range to be met.
- Some bands saturate a little early in blue FPA; this was expected.
- Reduced dynamic range from 660nm-715nm to increase SNR for FLH product (and at 1038nm for atm. cor.).

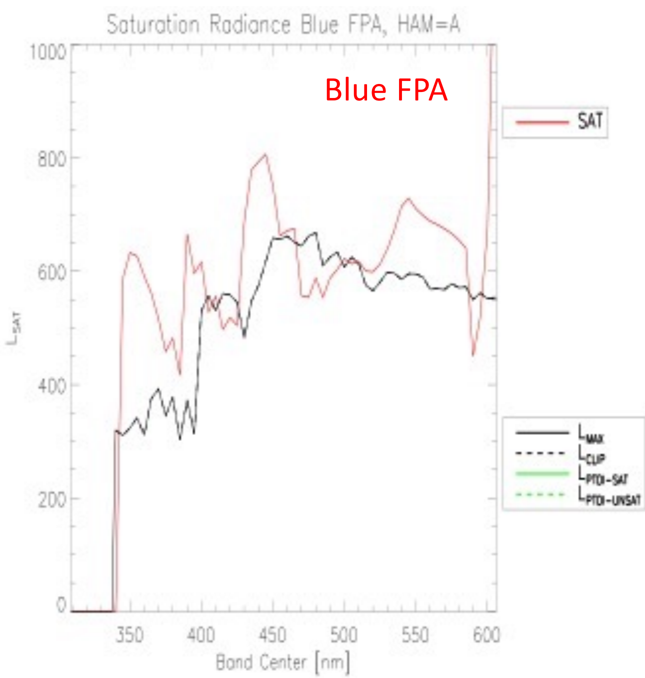

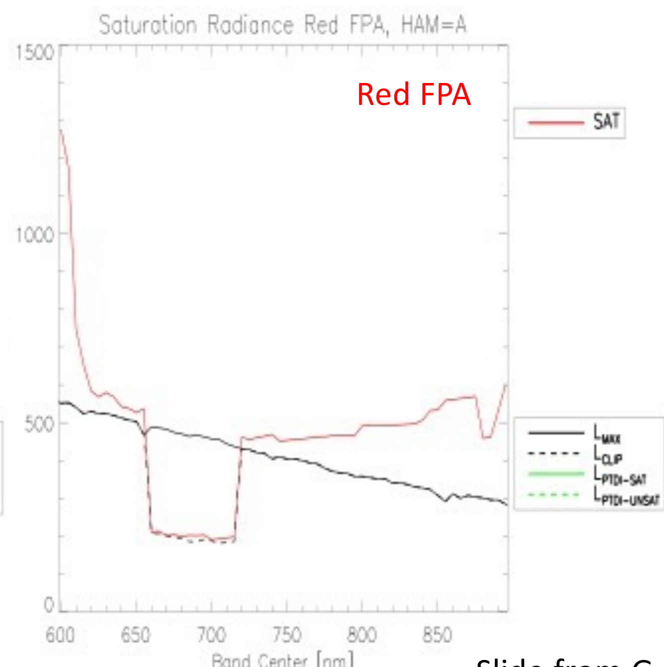

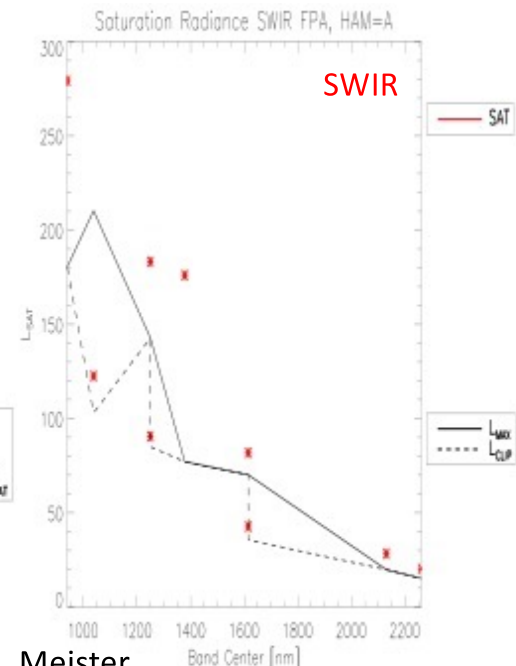

Slide from G. Meister, IGARSS 2023.

SWIR band hysteresis

- Due to SWIR band detector and electronics characteristics, significant hysteresis is observed after a strong radiance gradient (e.g. cloud/ocean boundary)
- We developed a correction for ETU that reduces the impact to within the noise 3 pixels after the radiance transition (see below for example; red line is 1km x1km stimulus)
- Effect is expected to be linear and to follow the superposition principle, so we expect good performance of the flight unit correction with real on-orbit data

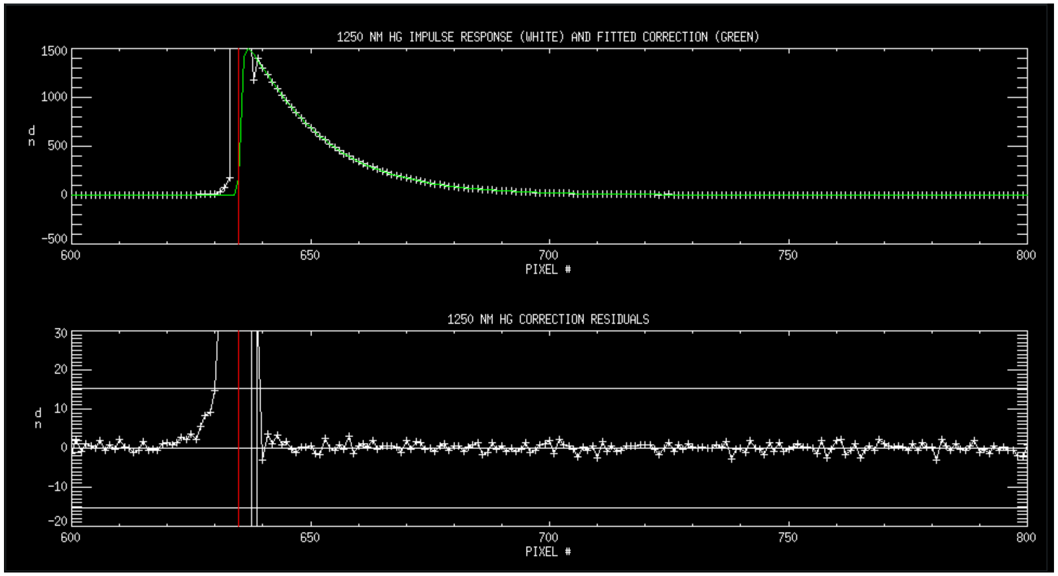

Hysteresis will be monitored on-orbit via lunar measurements (stare mode) and a dedicated on-board device (SPCA: Solar Pulse calibration Assembly)

Slide from G. Meister, IGARSS 2023.

Absolute uncertainty estimate for OCI top-of-atmosphere radiance using solar diffuser calibration (preliminary):

865nm	940nm	1038nm	1250nm HG (Ocean)	1250nm SG	1378nm	1615nm HG (Ocean)	1615nm SG	2130nm	2260nm Ocean	2260nm Cloud
0.72%	1.78%	1.40%	1.42%	2.06%	2.01%	1.80%	2.31%	2.90%	2.50%	2.95%

400-885nm: similar to 865nm estimate
350nm-400nm: closer to 2%
315nm-350nm: undetermined (‘goal’ bands, prelaunch light sources often not bright enough)

Summary

- Testing of OCI after integration to Spacecraft completed in October 2023;
- PACE launched Februrary 8th 2024
- PACE/OCI currently in commissioning phase (until end of March/early April)
- OCI will provide lunar irradiance measurements at +/-7deg phase angles to track long term radiometric gain changes
- Hyperspectral from 315nm to 885nm, 7 bands from 940nm-2260nm
- Spatial resolution similar to SeaWiFS
- Absolute calibration accuracy about 1% below 900nm, potentially useful to improve spectral interpolation of current lunar irradiance models
- OCI will perform ‘lunar stare’ measurements for SWIR hysteresis monitoring

Backup

SNR at L_{TYP} for multispectral bands

Comparison of different SNR estimates over TVAC tests (HAM A shown; HAM B is consistent).
All multispectral and SWIR bands well above the baseline requirement.

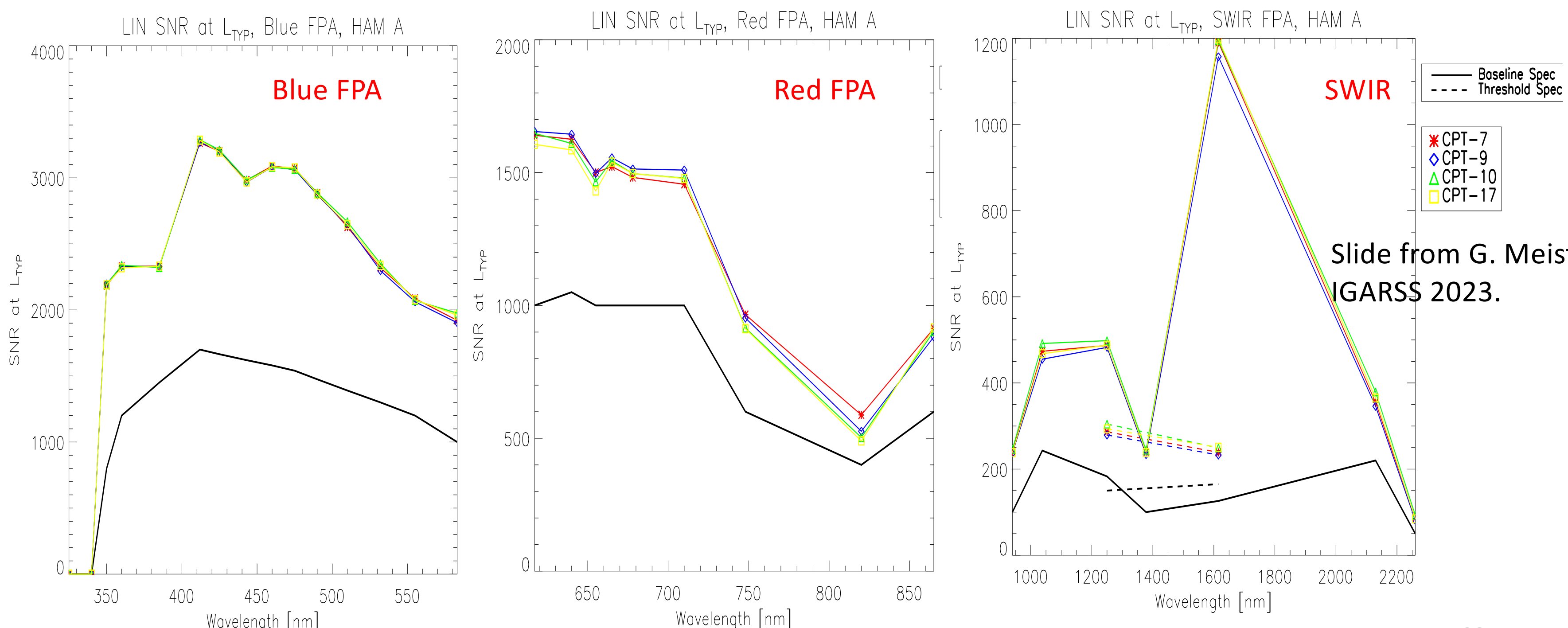

Slide from G. Meister, IGARSS 2023.

Selected OCI publications:

- - Jeff McIntire, Samuel Kitchen-McKinley, Hyeungu Choi, Gerhard Meister, "Progressive TDI measurements with the PACE OCI ETU," Proc. SPIE 11829, Earth Observing Systems XXVI, 118290S (1 August 2021); https://doi.org/10.1117/12.2594239

- Eugene Waluschka, Nicholas R. Collins, William B. Cook, Eric T. Gorman, George M. Hilton, Joseph J. Knuble, Gerhard Meister, Jeffrey W. McIntire, "PACE Ocean Color Instrument polarization testing and results," Proc. SPIE 11829, Earth Observing Systems XXVI, 118290R (1 August 2021); https://doi.org/10.1117/12.2594029

- Samuel Kitchen-McKinley, Jeff McIntire, Hyeungu Choi, Gerhard Meister, "PACE OCI pre-launch ETU spectral characterization and performance," Proc. SPIE 11829, Earth Observing Systems XXVI, 118290Q (1 August 2021); https://doi.org/10.1117/12.2594306

- Gerhard Meister, Joseph J. Knuble, William B. Cook, Eric T. Gorman, P. Jeremy Werdell, "Calibration plan for the Ocean Color Instrument (OCI) engineering test unit," Proc. SPIE 11151, Sensors, Systems, and Next-Generation Satellites XXIII, 111511W (10 October 2019); https://doi.org/10.1117/12.2550820

- Jeff McIntire, Sam Kitchen-McKinley, Dan Todaro, Gerhard Meister, "Simulating response versus scan angle characterization on OCI for the upcoming PACE mission," Proc. SPIE 11151, Sensors, Systems, and Next-Generation Satellites XXIII, 111511D (10 October 2019); https://doi.org/10.1117/12.2532782

- Gorman, E., D. A. Kubalak, P. Deepak, et al. 2019. "The NASA Plankton, Aerosol, Cloud, ocean Ecosystem (PACE) mission: an emerging era of global, hyperspectral Earth system remote sensing." Sensors, Systems, and Next-Generation Satellites XXIII 11151 111510G [10.1117/12.2537146]

- Gerhard Meister, Joseph J. Knuble, Leland H. Chemerys, Hyeungu Choi, Nicholas R. Collins, Robert E. Eplee, Ulrik Gliese, Eric T. Gorman, Kim Jepsen, Samuel Kitchen-McKinley, Shihyan Lee, Jeffrey W. Mcintire, Frederick S. Patt, Bradley C. Tse, Eugene Waluschka, P. Jeremy Werdell, "Test Results from the Prelaunch Characterization Campaign of the Engineering Test Unit of the Ocean Color Instrument of NASA's Plankton, Aerosol, Cloud and Ocean Ecosystem Mission" Front. Remote Sens., 23 June 2022 Sec. Multi- and Hyper-Spectral Imaging https://doi.org/10.3389/frsen.2022.875863.

- J.Werdell; M. Behrenfeld; P. Bontempi; E. Boss; B. Cairns; G. Davis; B. Franz; U. Gliese; E. Gorman; O. Hasekamp; K. Knobelspiesse; A. Mannino; V. Martins; C. McClain; G. Meister; L. Remer, "The Plankton, Aerosol, Cloud, ocean Ecosystem (PACE) mission: Status, science, advances." Bulletin of the American Meteorological Society 100 (9): 1775–1794, 2019, doi: 10.1175/bams-d-18-0056.1.

Selected OCI publications (continued):

- Shihyan Lee, Gerhard Meister, Samuel Kitchen-McKinley, Joseph Knuble, Ulrik Gliese, Robert Bousquet, "PACE OCI crosstalk characterization based on pre-launch testing," Proc. SPIE 12729, Sensors, Systems, and Next-Generation Satellites XXVII, 1272919 (19 October 2023); https://doi.org/10.1117/12.2677567

- Joseph J. Knuble, Gerhard Meister, Hyeungu Choi, Nicholas R. Collins, Kim Jepsen, Shihyan Lee, Jim McCarthy, Robert Bousquet, William B. Cook, Colby Jurgenson, Ulrik Gliese, Eric T. Gorman, "Measurement techniques for the high-contrast and in-field stray light performance of OCI," Proc. SPIE 12729, Sensors, Systems, and Next-Generation Satellites XXVII, 127290P (19 October 2023); https://doi.org/10.1117/12.2682126

- U. Gliese, Z. Rhodes, K. Squire, K. S. Jepsen, B. Cairns, B. L. Clemons, J. Cook, R. Esplin, R. H. Estep Jr., E. T. Gorman, E. Kan, G. Meister, W. Lu, D. B. Mott, F. S. Patt, J. Peterson, R. G. Schnurr, "Pulse response of the shortwave infrared detection system of the ocean color instrument for the NASA PACE Mission," Proc. SPIE 12729, Sensors, Systems, and Next-Generation Satellites XXVII, 127290O (19 October 2023); https://doi.org/10.1117/12.2684367

- Robert E. Eplee Jr., Gerhard Meister, Shihyan Lee, Kenneth J. Squire, Ulrik Gliese, Joseph J. Knuble, Deepak Patel, "Prelaunch radiometric calibration of the thermal response of the PACE Ocean Color Instrument," Proc. SPIE 12685, Earth Observing Systems XXVIII, 1268509 (4 October 2023); https://doi.org/10.1117/12.2677463

- Jeff McIntire, Eugene Waluschka, Gerhard Meister, Joseph Knuble, William B. Cook, "PACE OCI polarization sensitivity based on pre-launch testing," Proc. SPIE 12685, Earth Observing Systems XXVIII, 126850C (4 October 2023); https://doi.org/10.1117/12.2677522

- Samuel Kitchen-McKinley, Jeff McIntire, Hyeungu Choi, Gerhard Meister, Julia Barsi, Brendan McAndrew, Andrei Sushkov, Barbara Zukowski, William B. Cook, Ulrik Gliese, Kenneth Squire, Joseph Knuble, "Pace OCI Flight Unit Pre-Launch Spectral Characterization," IGARSS 2023 - 2023 IEEE International Geoscience and Remote Sensing Symposium, Pasadena, CA, USA, 2023, pp. 1349-1352, doi: 10.1109/IGARSS52108.2023.10283202.

- G. Meister et al., "Initial Look at the Results from the Prelaunch Characterization Campaign of OCI on the Pace Mission," IGARSS 2023 - 2023 IEEE International Geoscience and Remote Sensing Symposium, Pasadena, CA, USA, 2023, pp. 1345-1348, doi: 10.1109/IGARSS52108.2023.10281727.

- U. Gliese, D.A. Kubalak, C.R. Auletti, S.R. Babu, B. Blagojevic, K. Boggs, R.R. Bousquet, G. Bredthauer, G.L. Brown, N.T. Cao, T.L. Capon, J. Champagne, L.H. Chemerys, F.N. Chi, B.L. Clemons, J. Cook, W.B. Cook, N.P. Costen, K.R. Dahya,P.V. Dizon, R. Esplin, R.H. Estep, Jr., A.R. Feizi, S.H. Feng, E.T. Gorman, J.A. Guzek, O.A. Haddad, C.F. Hakun, L.B. Haynes, M.J. Hersh, C.S. Hill, D.G. Holliday, L.A. Ramos-Izquierdo, K.S. Jepsen, E. Kan, B.P. Kercheval, S. Kholdebarin, J.J. Knuble, A.T. La, E.D. Laurila, M.R. Lin, W. Lu, A.J. Mariano, L.A. Meier, G. Meister, B. Monosmith, D.B. Mott, M.M. Mulloney, Q.V. Nguyen, T.J. Nolan, M.A. Owens, J. Peterson, M.A. Quijada, K.A. Ray, Z. Rhodes, K. Squire, C.P. Stull, J. Thomes, E. Waluschka, Y. Wen, M.E. Wilson, and P.J. Werdell, "Optical and Detector Design of the Ocean Color Instrument for the NASA Pace Mission," IGARSS 2023 - 2023 IEEE International Geoscience and Remote Sensing Symposium, Pasadena, CA, USA, 2023, pp. 1337-1340, doi: 10.1109/IGARSS52108.2023.10281729.

- Joseph J. Knuble, Gerhard Meister, Leland H. Chemerys, et al., "Pre-Launch Calibration Methods of OCI on the Pace Mission," IGARSS 2023 - 2023 IEEE International Geoscience and Remote Sensing Symposium, Pasadena, CA, USA, 2023, pp. 1341-1344, doi: 10.1109/IGARSS52108.2023.10282804.

- Hyeungu Choi, Jeff McIntire, Samuel Kitchen-McKinley, Gerhard Meister, Leland Chemerys, Shihyan Lee, "Spatial characterization of PACE OCI ETU using time-delay mode," Proc. SPIE 12232, Earth Observing Systems XXVII, 1223211 (30 September 2022); https://doi.org/10.1117/12.2632640

- Kenneth J. Squire, Jacob K. Hedelius, David K. Moser, James Q. Peterson, Eric T. Gorman, Emily Kan, D. Brent Mott, Ulrik B. Gliese, Gerhard Meister, "PACE OCI short-wave infrared detection assembly frequency-dependent linearity characterization and uncertainty analysis," Proc. SPIE 12232, Earth Observing Systems XXVII, 1223212 (30 September 2022); https://doi.org/10.1117/12.2633617

- Jacob K. Hedelius, Kenneth J. Squire, James Q. Peterson, Branimir Blagojević, Ulrik B Gliese, Eric T. Gorman, David K. Moser, Zakk Rhodes, Pedro Sevilla, Gerhard Meister, "Infrared spectral responses of the Ocean Color Instrument (OCI) pre-assembly and integration," Proc. SPIE 12232, Earth Observing Systems XXVII, 1223210 (30 September 2022); https://doi.org/10.1117/12.2631201